

## **Development of a Methodology for Analysis of the Impact of Modifying Neutron Cross Sections**

Michael T. Wenner<sup>1\*</sup>, Alireza Haghghat<sup>1</sup>, James M. Adams<sup>2</sup>, Allan D. Carlson<sup>2</sup>,  
Steven M. Grimes<sup>3</sup>, Thomas N. Massey<sup>3</sup>

<sup>1</sup>*Department of Nuclear and Radiological Engineering, University of Florida, Gainesville, FL 32611*

<sup>2</sup>*National Institute of Standards and Technology, Gaithersburg, MD 20899*

<sup>3</sup>*Institute of Nuclear and Particle Physics, Department of Physics and Astronomy, Ohio University, Athens, OH 45701*

Monte Carlo analysis of a Time-of-Flight (TOF) experiment can be utilized to examine the accuracy of nuclear cross section data. Accurate determination of this data is paramount in characterization of reactor lifetime. We have developed a methodology to examine the impact of modifying the current cross section libraries available in ENDF-6 format (1) where deficiencies may exist, and have shown that this methodology may be an effective methodology for examining the accuracy of nuclear cross section data. The new methodology has been applied to the iron scattering cross sections, and the use of the revised cross sections suggests that reactor pressure vessel fluence may be underestimated.

***KEYWORDS: Iron Cross Section, Fe-56, scattering, pressure vessel fluence***

### **1. Introduction**

Through Monte Carlo analyses of TOF experiments, we have identified possible deficiencies in the Fe-56 scattering cross section. (2) Accurate determination of the fast-neutron fluence at the pressure vessel has been accomplished by performing neutron transport calculations. Clearly, the safe design and operation of nuclear systems are largely dependent on the nuclear data used in these calculations. This paper discusses the development of a methodology for analysis of the impact of modifying iron (i.e. Fe-56) scattering cross sections.

### **2. Background**

Experimental data were obtained via a neutron spectroscopy technique, known as time-of-flight (TOF), using the spherical-shell transmission method. All experimental work was performed at the Ohio University accelerator laboratory. (3) Iron shells are employed with different thicknesses, and neutron TOF spectra are obtained. A schematic of the experimental facilities is given in Fig. 1 which shows the beam swinger that allows angular distributions of the outgoing neutrons to be measured without moving the neutron detector.

---

\* Corresponding author, Tel. 352-392-1401 Ext. 332, FAX 352-392-3380, E-mail: mtw125@ufl.edu

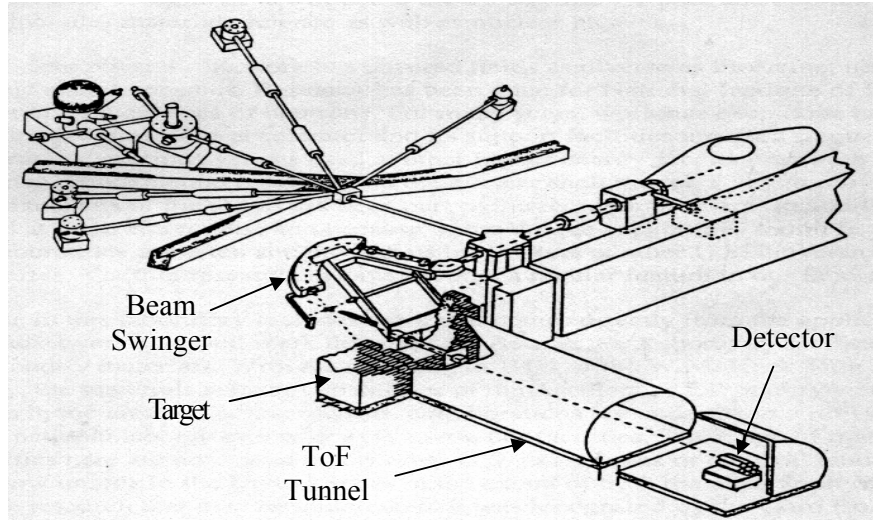


**Fig. 1** Experimental Facilities Schematic

A procedure was developed to utilize the experimental data to generate a Monte Carlo source distribution. In Ref. 2, we have studied the validity of this source with different neutron source reactions. Neutron sources were generated based on 3 MeV, 5 MeV and 7 MeV incident deuterons with the  $D(d,n)$  source reaction as well as 5.1 MeV incident protons with the  $^{15}N(p,n)$  reaction. For each incident particle energy and neutron source reaction, measurements were made at several different angles to provide data about the neutron angular source spectrum. Each of these measurements provides a spectrum which covers a range of neutron energies. For the NE-213 detector measurements, a spherical shell target of 8 cm thickness was used for all the sources. In addition, for that detector, measurements were made with a smaller sphere of ~3cm thickness with the  $^{15}N(p,n)$  source reaction. (4) These thicknesses were chosen to optimize the effect of neutron inelastic scattering. (5) Analysis of these data exhibited discrepancies that may be attributed to the inaccuracies of the Fe-56 scattering cross section.

### 3. Comparison of Calculation and Experiment

The results of the calculations identified possible discrepancies between experiment and calculation in several small energy regions. Given that the source distribution generated and MCNP model are accurate, the differences observed between the calculation and experimental spectra can be caused by computational statistical errors, experimental errors, and the error in the iron scattering cross sections. Accounting for the first two components of the error (differences), the remaining differences can be attributed to the error in the iron scattering cross sections that are used. These errors for the large sphere are given in Table 1.

**Table 1** Observed Error and the Associated Energy Bin

Interaction	Energy Bin (MeV)	(%) Change in Inelastic Cross Section
3 MeV incident d, $D(d,n)$	6.153 - 6.203	~8
5 MeV incident d, $D(d,n)$	8.155 - 8.205	~13
7 MeV incident d, $D(d,n)$	10.756 - 10.806	~18

From the data given in Table 1, a trend is observed which shows an increasing difference with increasing energy. For this reason, the iron scattering cross sections are modified by increasing percentages for increasing energies.

#### 4. Cross Section Modification

A utility code (XSMOD) (6) was developed in FORTRAN-90 for modifying neutron cross sections in ENDF-6 format which depend on energy. XSMOD includes capabilities for modifying cross sections for any MT number given. Input for XSMOD is in the form of an extracted material (MAT) from the ENDF data tape.

XSMOD proceeds after initialization by reading in all cross sections in the cross section file (File 3). XSMOD prompts the user for pertinent input. Although all cross sections are read, currently only the cross sections listed in the cross section modifier menu may be modified directly. These reactions are presented in Fig. 2.

```

                                     XS MODIFIER MENU
Which XS would you like to modify?
TOTAL XS                               1
TOTAL ELASTIC XS                       2
TOTAL NONELASTIC XS                   3
NONELASTIC XS BY PARTS                 3
TOTAL INELASTIC XS                     4
INELASTIC XS BY PARTS                  4
TOTAL FISSION XS                       18
FISSION XS BY PARTS                    18
NEUTRON DISAPPEARANCE XS               101
NEUTRON DISAPPEARANCE XS BY PARTS     101
TO CONTINUE                             0
```

Fig.2 XSMOD Cross Section Modifier Menu

As shown in Figure 2, there are several options for cross sections to be modified “by parts”. This refers to cross sections in the cross section modifier menu which can be derived from lower level cross sections such as the inelastic scattering cross section which is often derived from the sum of discrete level excitation cross section (MT=51-90), and continuum inelastic scattering (MT=91).

After selecting the cross section to be modified, the number of energy intervals and energy ranges to be modified are given. Modifications are made by one of two ways. Either a constant change or a percent change in each of the point-wise cross section data within the energy interval of interest.

#### 4.1 Cross Section Rebuilding

Upon making appropriate cross section changes, cross sections can then be rebuilt (except elastic) by a sum of their parts, or arrived at by decomposing of other cross sections (only elastic). Cross sections that can be rebuilt are shown in Figure 3.

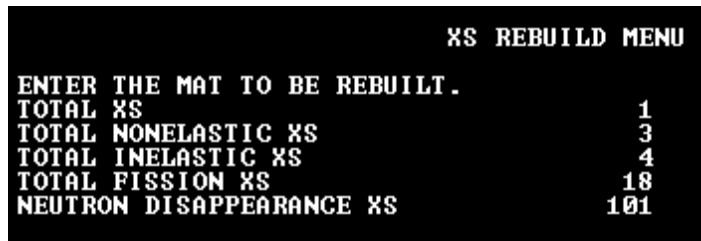


Fig.3 XSMOD Cross Section Rebuild Menu

The ENDF data mostly are given as lists of values on a defined grid with an interpolation law to obtain the values between the grid points. Since partial cross sections' point-wise energy grids do not always match the derived cross section energy grids, interpolation may be necessary. For this reason, ENDF-6 formats require information about recommended interpolation schemes to use for all data points given in each cross section to retain the highest accuracy. The available interpolation schemes used in ENDF are listed in Table 2.

Table 2 ENDF-6 Interpolation Schemes

INT	Interpolation Scheme
1	y is constant in x (constant, histogram)
2	y is linear in x (linear-linear)
3	y is linear in ln(x) (linear-log)
4	ln(y) is linear in x (log-linear)
5	ln(y) is linear in ln(x) (log-log)
6	Special one-dimensional interpolation law, used for charged-particle cross sections only
11 – 15	Method of corresponding points (follow interpolation laws of 1-5)
21 – 25	Unit base interpolation (follow interpolation laws of 1-5)

Currently, XSMOD is capable of using interpolation (INT) of types 2, 3, 4 and 5. These schemes were tested by using the rebuild feature without making cross section changes, comparing input cross sections to rebuilt cross section. For example, when rebuilding the Fe-56 total cross section, a maximum error of 0.00648% was observed.

#### 4.2 Determination of Elastic Scattering Component

The elastic scattering cross section is often obtained by subtracting the non-elastic cross section from the total cross section. It is important to note that when energy grids for the total cross section and non-elastic cross sections are not identical, interpolation is used to obtain cross sections at the necessary locations for subtraction.

Using this procedure of rebuilding and subtracting, one can obtain new cross sections in a variety of ways. Maximum observed error for obtaining the elastic scattering cross section component when using the iron cross section with no changes in cross section was 0.108%. It is important to note that at this point, the cross section value was comparatively small causing this error to be significantly larger than the error observed in the rest of the cross section values.

The XSMOD program output is in the form of two files. One file contains all the rebuilt and decomposed cross sections, along with the input cross section data, and their corresponding

point-wise energy in tabular form. This file is useful for plotting. The second file contains an updated version of the input cross section for the cross section processed. This file is in the ENDF-6 format.

### 4.3 Modification Testing

Shown in this section are figures obtained from XSMOD modified cross sections. These figures show changes of cross sections used for testing purposes. Figures 4 - 7 show resulting cross sections obtained from changing the inelastic scattering by increasing it a relative amount of 75% in the energy range of 1.75 MeV to 2.25 MeV. To compensate for this change, the elastic cross section is modified correspondingly such that the total cross section is conserved.

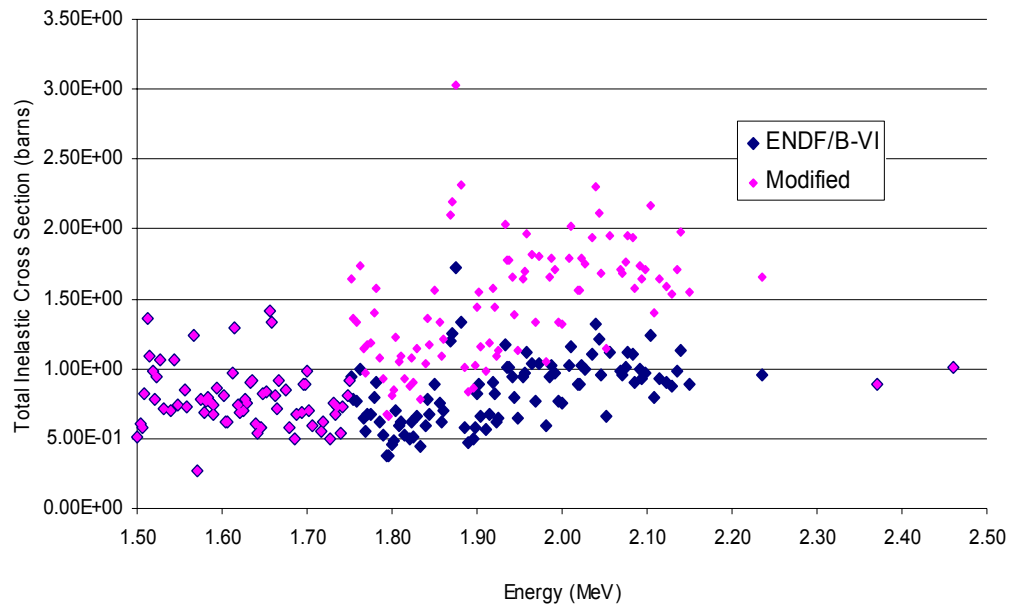


**Fig.4** Fe-56 Inelastic Cross Section Modification Comparison

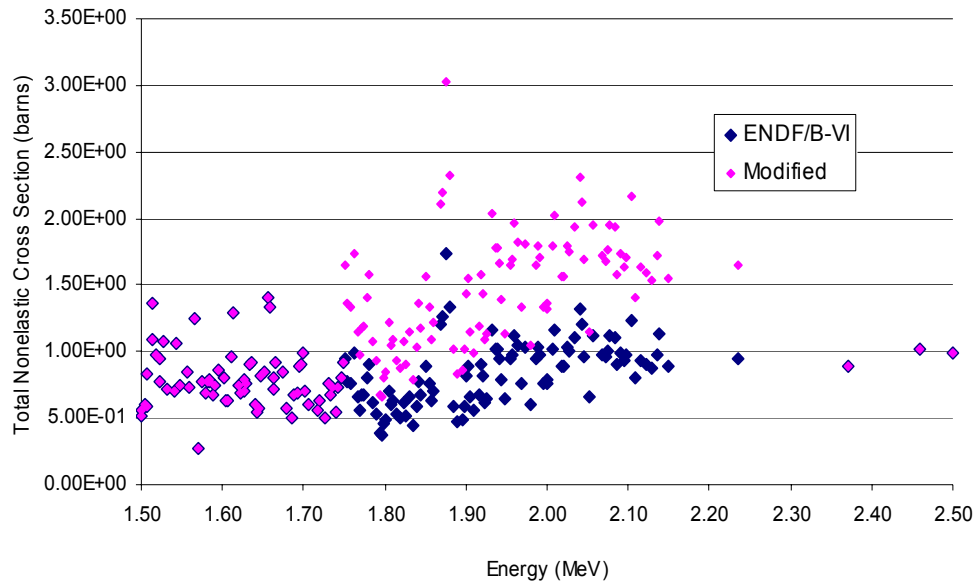


**Fig.5** Fe-56 Non-elastic Cross Section Modification Comparison

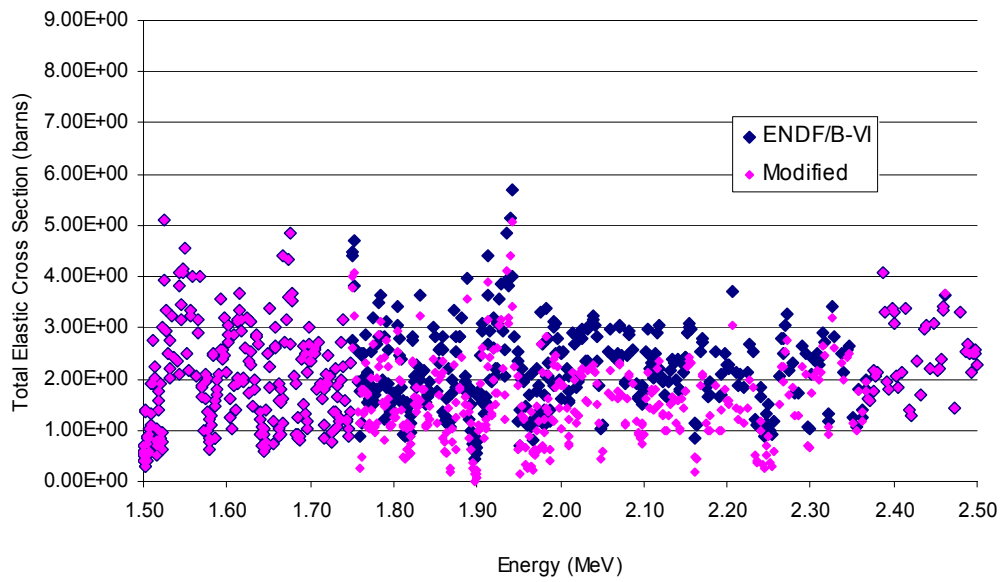


**Fig.6** Total Fe-56 Elastic Cross Section Modification Comparison

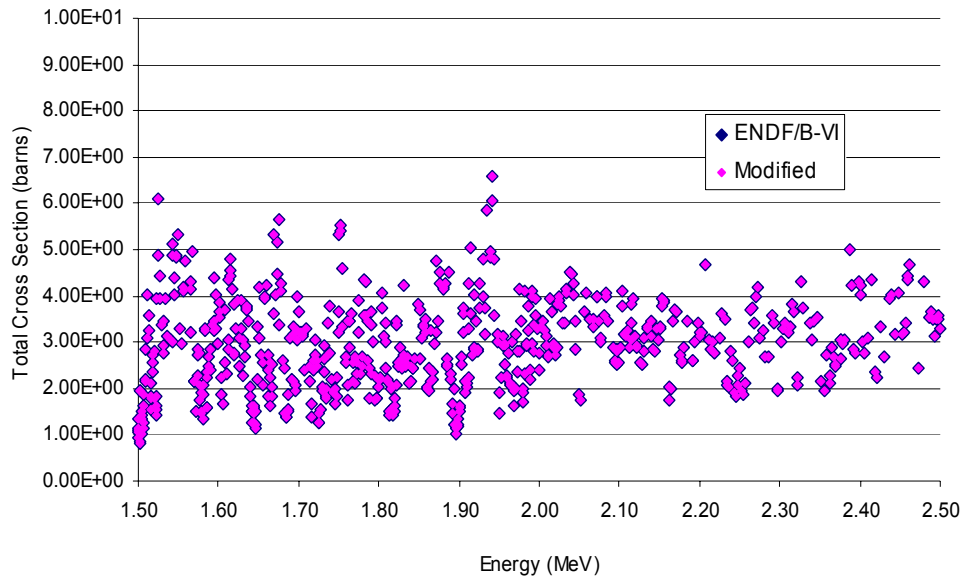


**Fig.7** Fe-56 Total Cross Section Modification Comparison

Figures 4 - 5 show an increase between 1.75 MeV and 2.25 MeV for inelastic and non-elastic cross sections, while Figure 6 shows a decrease in the elastic cross section in order to conserve the total cross section. Figure 7 shows that the total cross section remains constant

#### 4.4 Actual Modifications

The XSMOD code was utilized to modify cross sections in energy corresponding to the energy bins in Table 1. A larger difference between experiment and calculation was observed with increasing source energy as given in Table 1.

With the increasing differences observed, the Fe-56 inelastic cross section was decreased by greater amounts corresponding to the energy regions shown for the peak regions as seen in Table 2. During cross section modification, the total cross section is kept constant and the changes in the inelastic cross section are compensated by increasing the elastic cross section. Modifications are made in the entire energy region of interest by the same percentage by modifying the point-wise data located in that region.

**Table 2** Cross Section Adjustments and Their Associated Energy Bin

Interaction	Energy Bin (MeV)	(%) Change in Inelastic Cross Section
3 MeV incident d, D(d,n)	6.153 - 6.203	-21
5 MeV incident d, D(d,n)	8.155 - 8.205	-29
7 MeV incident d, D(d,n)	10.756 - 10.806	-35

To examine the effect of the adjusted cross sections, both continuous energy and multigroup cross sections were generated. NJOY (7) was utilized to generate continuous energy cross sections for the MCNP code in ACE format, while a multigroup library was generated utilizing the methods described in Reference (8).

## 5. Results

The calculated spectra based on the adjusted cross sections are closer to the experimental predictions in the peak regions. Relative differences were reduced to ~3.5%, ~8% and ~11% for 3 MeV, 5 MeV and 7 MeV incident deuterons, respectively. Figure 8 shows the results for the 3 MeV case. These results indicate a reduction of differences by ~40%.

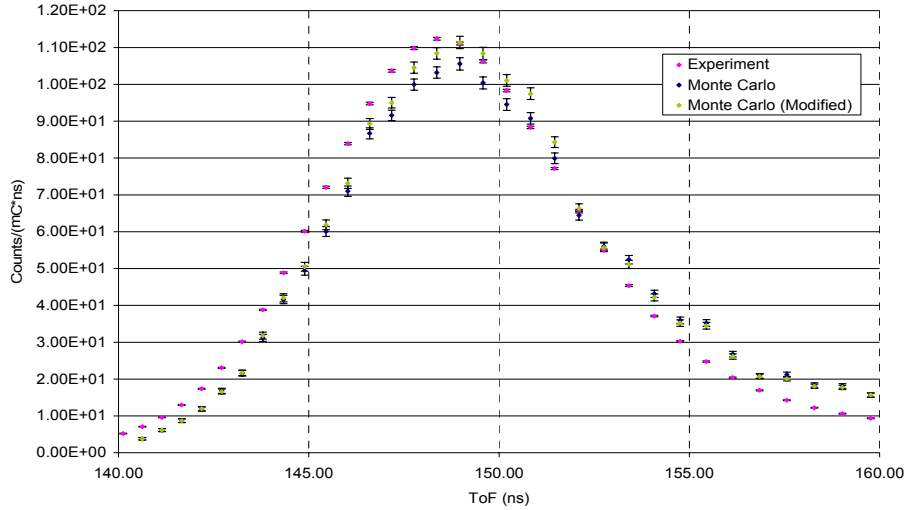


**Fig.8** Comparison of Modified D(d,n) reaction Monte Carlo Calculations and Experimental Data for 3 MeV incident deuterons and the 0 Degree Angle (Peak Region)

To test the multigroup cross sections, a 1-D reactor pressure vessel (PV) model was simulated corresponding to Figure 9.

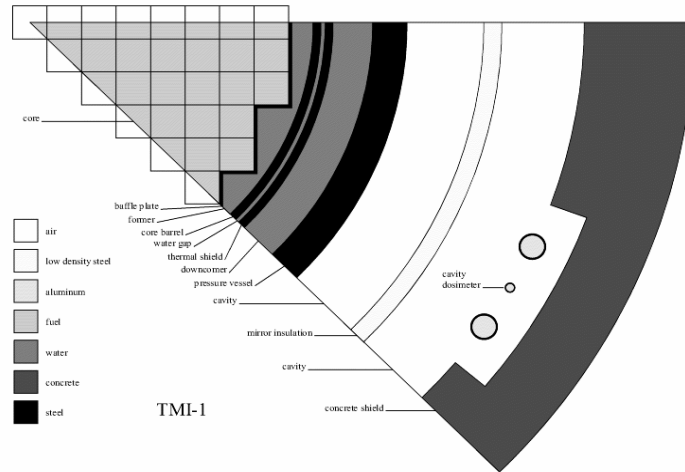


**Fig.9** Reactor Pressure Vessel Model

Results were obtained from multigroup cross sections collapsed from the original ENDF/B-VI data and the adjusted cross sections. Reaction rates for the  $^{63}\text{Cu}(n,\alpha)$ ,  $^{54}\text{Fe}(n,p)$ ,  $^{58}\text{Ni}(n,p)$ ,  $^{46}\text{Ti}(n,p)$ ,  $^{237}\text{Np}(n,f)$ , and  $^{238}\text{U}(n,f)$  interactions were determined at the cavity dosimeter and compared to the test results obtained from the library derived from the original ENDF/B-VI library. Table 3 gives the reaction rate ratios (ENDF/B-VI/adjusted cross section) for the six interactions. Given that the adjusted cross sections were in better agreement with experiment, we can see from the data in Table 3 that the model predicts the neutron fluence will

increase based on these changes.

**Table 3** Reaction Rate Ratios (ENDF/B-VI/Adjusted Cross Section) at the Cavity Dosimeter

Interaction	Threshold Energy (MeV)	$\frac{ENDF / B - VI}{Adjusted}$
$^{63}\text{Cu}(n,\alpha)$	1.71	.9410
$^{54}\text{Fe}(n,p)$	2.8	.9862
$^{58}\text{Ni}(n,p)$	0.5	.9877
$^{46}\text{Ti}(n,p)$	2.97	.9627
$^{237}\text{Np}(n,f)$	0.1	.9986
$^{238}\text{U}(n,f)$	0.5	.9958

## 6. Conclusion

We conclude that this procedure can be effectively utilized to provide information about the accuracy of nuclear cross section data. Our findings indicate that Pressure Vessel fluences might be underestimated based on the currently available libraries. This would be a very important issue for the reactor material integrity and lifetime. Future studies are needed.

## Acknowledgements

The authors wish to acknowledge support for this project by the U.S. Department of Energy NERI program.

## References

- 1) McLane, V., "ENDF-102 Data Formats and Procedures for the Evaluated Nuclear Data File ENDF-6", BNL-NCS-44945-01/04-Rev. Informal Report, Brookhaven National Laboratory, (2001).
- 2) Wenner, Michael, et al., "Monte Carlo Modeling of a Time of flight Experiment", This Conference
- 3) R. W. Finlay, C. E. Brient, D. E. Carter, et al., "The Ohio University beam swinger facility," Nucl Inst & Meth., 198, 197 (1982).
- 4) Gardner, S., Haghigat, A., and Patchimpattapong, A., "Monte Carlo Analysis of Spherical Shell Transmission Experiment with New Tallying Methodology, presented at M&C 2001 – ANS Topical Meeting, Salt Lake City, Utah (2001).
- 5) S. Gardner, A. Haghigat, A. Patchimpattapong, J. Adams, A. Carlson, S. Grimes, T. Massey, "A new Monte Carlo tallying methodology for optimizing the NERI spherical-shell transmission experiment," Trans. American Nucl. Soc., 84, 154 (2001).
- 6) Wenner, Michael, "Development of a Monte Carlo Methodology for Investigation of Neutron Cross Sections with a Time of Flight Experiment," M.S. Thesis, Nuclear Engineering, The Pennsylvania State University, (2003).
- 7) R. E. MacFarlane and R. M. Boicourt, "NJOY: A Neutron and Photon Processing System," Trans. Am. Nucl. Soc. 22, 720 (1975).
- 8) Alpan, F. A., Haghigat, A., "Advanced Methodology for Selecting Group Structures for Multigroup Cross Section Generation," Proceedings of PHYSOR 2000 – ANS International Topical Meeting on Advances in Reactor Physics and Mathematics and Computation into the Next Millenium, May 7-23, 2000, on CD, Pittsburgh, PA.